

# Comparative first-principles analysis of the absorption spectra of $\text{ZnAl}_2\text{S}_4$ and $\text{ZnGa}_2\text{O}_4$ crystals doped with $\text{Cr}^{3+}$

M.G. Brik<sup>a</sup>

Department of Chemistry, School of Science and Technology, Kwansai Gakuin University, 2-1 Gakuen, Sanda, Hyogo 669-1337, Japan

Received 6 October 2005 / Received in final form 21 October 2005

Published online 10 March 2006 – © EDP Sciences, Società Italiana di Fisica, Springer-Verlag 2006

**Abstract.** Systematic first-principles analysis of the energy level schemes and ground state absorption spectra of trivalent chromium in  $\text{ZnAl}_2\text{S}_4$  and  $\text{ZnGa}_2\text{O}_4$  crystals has been performed in the present paper. The recently developed first-principles approach to the analysis of the absorption spectra of impurity ions in crystals based on the discrete variational multi-electron (DV-ME) method [K. Ogasawara et al., Phys. Rev. B **64**, 115413 (2001)] was used in the calculations. The method is based on the numerical solution of the Dirac equation; no phenomenological parameters are used in the calculations. As a result, complete energy level schemes of the  $\text{Cr}^{3+}$  ion and its absorption spectra in both crystals were calculated, assigned and compared with experimental data. By performing analysis of the molecular orbital (MO) population, it was shown that the covalency of the chemical bonds between the  $\text{Cr}^{3+}$  and  $\text{S}^{2-}$  ions is more significant than that one between the  $\text{Cr}^{3+}$  and  $\text{O}^{2-}$  ions.

**PACS.** 71.15.Rf Relativistic effects – 71.70.Ch Crystal and ligand fields – 71.70.Ej Spin-orbit coupling, Zeeman and Stark splitting, Jahn-Teller effect

## 1 Introduction

A large class of compounds exhibits the spinel structure, the general chemical formula of which can be written as  $\text{AB}_2\text{X}_4$ . They crystallize in the cubic  $\text{Fd}3\text{m}$  space group; the total number of representatives of this class is 140 [1]. Both title hosts belong to this class as well; their lattice constants are 8.3358 Å for  $\text{ZnGa}_2\text{O}_4$  [2] and 10.009 Å for  $\text{ZnAl}_2\text{S}_4$  [3].  $\text{Cr}^{3+}$  ions substitute for  $\text{Ga}^{3+}$  and  $\text{Al}^{3+}$  ions in octahedral coordination; the chemical bond lengths are 1.998 Å for  $\text{ZnGa}_2\text{O}_4$  and 2.410 Å for  $\text{ZnAl}_2\text{S}_4$ , respectively. Since electrical charges of both substituted and substituting ions are the same, no charge compensating addition is required to keep electrical neutrality of the crystals. Many experimental and semi-empirical studies of the  $\text{Cr}^{3+}$ -doped  $\text{ZnAl}_2\text{S}_4$  and  $\text{ZnGa}_2\text{O}_4$  can be found in the literature. For example, photoluminescence properties of  $\text{ZnAl}_2\text{S}_4:\text{Cr}^{3+}$  were studied in [4–6], magnetic susceptibility and luminescence were reported in [7], and electron paramagnetic resonance (EPR) measurements were published in [8,9]. Studies of the  $\text{ZnGa}_2\text{O}_4:\text{Cr}^{3+}$  optical spectra can be found in [10], investigations of the nearest  $\text{Cr}^{3+}$ -pairs interaction in  $\text{ZnGa}_2\text{O}_4$  were presented in [11]. Recently, an interest to  $\text{ZnGa}_2\text{O}_4:\text{Cr}^{3+}$  has been renewed due to its applications as nanosized phosphors [12–14].

In this paper we present the first-principles analysis of the energy level structure and absorption spectra of the  $\text{ZnAl}_2\text{S}_4:\text{Cr}^{3+}$  and  $\text{ZnGa}_2\text{O}_4:\text{Cr}^{3+}$  crystals based on the recently developed discrete variational multi-electron (DV-ME) method [15]. To the best of our knowledge, this is the first attempt of the first-principles calculations of the absorption spectra for the title hosts. We calculate the energy level schemes of  $\text{Cr}^{3+}$  ion in both crystals, model the absorption spectra, perform the population analysis of the calculated energy states, estimate numerically and compare the effects of the covalent bond formation between  $\text{Cr}^{3+}$  ions, on one hand, and  $\text{O}^{2-}$  and  $\text{S}^{2-}$  ions, on another hand, and discuss the comparison between the calculated and experimental results.

## 2 Method of calculations

We apply the fully-relativistic discrete-variational multi-electron (DV-ME) method, which is a configuration-interaction (CI) calculation program using the four-component fully-relativistic molecular spinors obtained by the discrete-variational Dirac-Slater (DV-DS) cluster calculations, developed by Ogasawara et al. [15]. The method is based on the numerical solution of the Dirac equation, and its main advantages are as follows: 1) the first-principles method without any phenomenological parameters (this is especially important for the development

<sup>a</sup> e-mail: brik@fukui.kyoto-u.ac.jp;  
brik@ksc.kwansei.ac.jp

of new materials, prediction of their expected properties and analysis of the common trends between similar compounds. It should be pointed out here, that the intrinsic feature of the method is the overestimation (by about 20–30%) of the absolute positions of the calculated energy levels. Later on we will refer to this phenomenon and suggest a way of improvement of the calculated results); 2) very wide area of applications: to any atom or ion in any symmetry from spherical to  $C_1$  for any energy interval from IR to X-ray; 3) possibility to take into account all effects of chemical bond formation, exchange and configuration interaction by numerical integration; 4) potential to calculate a wide variety of physical properties (such as transition probabilities, for example) using the obtained wave functions of the energy levels. All relativistic effects, such as spin-orbit interaction and dependence of mass on velocity, are no longer considered as small perturbations, but are taken into account from the very first step of calculations.

The key idea of the method is that the molecular orbitals (MO) consisting of the wave functions of an impurity ion and ligands are used throughout the calculations rather than atomic wave functions. This makes the effects of covalency to be taken into account explicitly, since the percentage contribution of wave functions of different ions to any MO can be readily evaluated. The many-electron wave functions are expressed as linear combination of the MO-based Slater determinants and the absorption peaks assignment can be done in terms of these Slater determinants. The relativistic many-electron Hamiltonian is written as follows (in atomic units)

$$H = \sum_{i=1}^n \left[ c\alpha \mathbf{p}_i + \beta c^2 - \sum_{\nu} \frac{Z_{\nu}}{|\mathbf{r}_i - \mathbf{R}_{\nu}|} + V_0(\mathbf{r}_i) + \sum_{\mu} \frac{Z_{\mu}^{eff}}{|\mathbf{r}_i - \mathbf{R}_{\mu}|} \right] + \sum_{i=1}^n \sum_{j>i}^n \frac{1}{|\mathbf{r}_i - \mathbf{r}_j|}, \quad (1)$$

where  $\alpha$ ,  $\beta$  are the Dirac matrices,  $c$  the velocity of light,  $\mathbf{r}_i$ ,  $\mathbf{p}_i$  the position and the momentum operator of the  $i$ th electron,  $Z_{\nu}$  and  $\mathbf{R}_{\nu}$  the charge and position of the  $\nu$ th nucleus,  $Z_{\mu}^{eff}$  and  $\mathbf{R}_{\mu}$  the effective charge and position of the  $\mu$ th ion outside the model cluster,  $n$  the number of explicitly treated electrons (in our case,  $3d$ -electrons of  $\text{Cr}^{3+}$ ).  $V_0(\mathbf{r}_i)$  is the potential from the remaining electrons [16]:

$$V_0 = \int \frac{\rho_0^G(\mathbf{r}')}{|\mathbf{r} - \mathbf{r}'|} d\mathbf{r}' + \frac{3}{4} \left[ \frac{\rho^G(\mathbf{r}) V_{xc} \{ \rho^G(\mathbf{r}) \} - \rho_0^G(\mathbf{r}) V_{xc} \{ \rho_0^G(\mathbf{r}) \}}{\rho_1^G(\mathbf{r})} - V_{xc} \{ \rho_1^G(\mathbf{r}) \} \right], \quad (2)$$

where  $\rho^G$ ,  $\rho_1^G$ ,  $\rho_0^G$  represent the charge density of all electrons, that of the explicitly treated electrons and that of the remaining electrons, respectively, and  $V_{xc}$  is the Slater's  $X_{\alpha}$  potential. The superscript  $G$  indicates

the values for the ground state. Diagonalization of the Hamiltonian (1) gives a complete electron energy level scheme for the considered cluster. Since the eigenfunctions are also obtained simultaneously, the absorption spectra (for electric dipole, electric quadrupole, and magnetic dipole transitions) can be obtained in a straightforward manner after calculating appropriate matrix elements (in fact, this is reduced to a numerical integration). For example, in the case of electric dipole transitions the oscillator strength (averaged over all possible polarizations) is calculated as follows:

$$I_{if} = \frac{2}{3} (E_f - E_i) \left| \left\langle \Psi_f \left| \sum_{k=1}^n \mathbf{r}_k \right| \Psi_i \right\rangle \right|^2, \quad (3)$$

where  $\Psi_i$  and  $\Psi_f$  are the initial and final states with energies of  $E_i$  and  $E_f$ , respectively. To emphasize the wide applicability of the method employed in the present paper, we mention that it has been successfully applied to the analysis of the  $\text{Cr}^{4+}$  absorption spectrum in  $\text{Y}_3\text{Al}_5\text{O}_{12}$  [17] and silicate crystals [18],  $4f - 4f$  absorption spectrum of  $\text{LiYF}_4:\text{Dy}^{3+}$  [19],  $4f - 5d$  absorption spectra of various trivalent lanthanides in  $\text{LiYF}_4$  [20,21], high lying energy  $4f$  and  $5d$  states of free trivalent lanthanides [22,23], calculations of the X-ray absorption near edge structure (XANES) spectra of transition metal ions [24–26].

### 3 Results of calculations and discussion

Octahedral  $[\text{CrS}_6]^{9-}$  and  $[\text{CrO}_6]^{9-}$  model clusters were used for calculations of the energy levels and absorption spectra. The Cartesian coordinates of ions (in Å) in both clusters obtained by using the crystal structure data from [2,3] are listed in Table 1. In order to take into account the effects of the surroundings of the above model clusters, an effective Madelung potential was considered by locating several thousand point charges (with charges “+3” for Ga, “+2” for Zn, “–2” for O in  $\text{ZnGa}_2\text{O}_4$  and “+3” for Al, “+2” for Zn, “–2” for S in  $\text{ZnAl}_2\text{S}_4$ ) at atomic sites outside the cluster. The number of the sampling points was 100 000 and the atomic orbitals used for the relativistic DV- $X_{\alpha}$  calculation were from  $1s$  to  $4p$  for  $\text{Cr}^{3+}$  ions, from  $1s$  to  $2p$  for  $\text{O}^{2-}$  ions and from  $1s$  to  $3p$  for  $\text{S}^{2-}$  ions.

In an octahedral crystal field the  $3d$  orbitals are split into  $t_{2g}$  and  $e_g$  orbitals, with the former being the ground state and the latter situated above it by  $10Dq$  [27] (for the sake of simplicity, irreducible representations of the  $O_h$  group are used at this point, and the existing deviations from this high symmetry are neglected, though the actual symmetry is used in all calculations). This allows to arrange 3  $d$ -electrons of the  $\text{Cr}^{3+}$  ion in these orbitals as shown in Table 2 (the number of Slater determinants for each configuration is shown as well).

Hamiltonian (1) was diagonalized in the space spanned by all 120 Slater determinants from the above table. The results of energy level calculations, in comparison with experimental data are shown in Table 3. Though complete

**Table 1.** Cartesian coordinates (in Å) of ions in the octahedral  $[\text{CrS}_6]^{9-}$  and  $[\text{CrO}_6]^{9-}$  model clusters (after [2,3]).

| Ions                                      | X        | Y        | Z        |
|---|----------|----------|----------|
| [CrS <sub>6</sub> ] <sup>9-</sup> cluster |          |          |          |
| Cr <sup>3+</sup>                          | 0        | 0        | 0        |
| S <sup>2-</sup>                           | -2.40589 | -0.09639 | 0.09639  |
| S <sup>2-</sup>                           | 0.09639  | 2.40589  | -0.09639 |
| S <sup>2-</sup>                           | 0.09639  | 0.09639  | -2.40589 |
| S <sup>2-</sup>                           | -0.09639 | -0.09639 | 2.40589  |
| S <sup>2-</sup>                           | 2.40589  | 0.09639  | -0.09639 |
| S <sup>2-</sup>                           | -0.09639 | -2.40589 | 0.09639  |
| [CrO <sub>6</sub> ] <sup>9-</sup> cluster |          |          |          |
| Cr <sup>3+</sup>                          | 0        | 0        | 0        |
| O <sup>2-</sup>                           | -0.09003 | -1.99392 | 0.09003  |
| O <sup>2-</sup>                           | 1.99392  | 0.09003  | -0.09003 |
| O <sup>2-</sup>                           | 0.09003  | 0.09003  | -1.99392 |
| O <sup>2-</sup>                           | -0.09003 | -0.09003 | 1.99392  |
| O <sup>2-</sup>                           | 0.09003  | 1.99392  | -0.09003 |
| O <sup>2-</sup>                           | -1.99392 | -0.09003 | 0.09003  |

**Table 2.** Distribution of electrons through the  $\text{Cr}^{3+}$   $3d$  orbitals ( $3d^3$  open shell) in the  $[\text{CrS}_6]^{9-}$  and  $[\text{CrO}_6]^{9-}$  model clusters.

| $t_{2g}$                     | $e_g$ | Number of Slater determinants |
|------------------------------|-------|-------------------------------|
| Ground state configuration   |       |                               |
| 3                            | 0     | 20                            |
| Excited state configurations |       |                               |
| 2                            | 1     | 60                            |
| 1                            | 2     | 36                            |
| 0                            | 3     | 4                             |

basis set consisting of 120 states was used in the calculations, only lowest states observed in experimental spectra are shown in both tables, for the sake of brevity. As mentioned in [21–23], there exists a systematic overestimation of the energy levels obtained by using the DV–ME method with respect to the experimental results; such an overestimation is also seen from the data of Table 3 for both clusters. This overestimation is about 20–30% and is due to underestimation of the electron correlation [21,22]. This discrepancy can be decreased by including high-lying electron configuration into the basis set, but this would lead to a significant increase of the dimension of Hamiltonian matrix and computation time. The calculated absorption spectrum is totally shifted to the higher energy region. If the *relative* positions of the absorption bands are of main importance, this overestimation can be left as is [21]. If, however, the *absolute* positions of the energy levels are to be obtained more precisely, one can *a posteriori* introduce a certain scaling factor [22,23,28], which minimizes the root-mean squared deviation between the calculated and experimental results. Such minimization was

performed for both considered crystals and the scaling factors were turned out to be 0.675 for  $\text{ZnAl}_2\text{S}_4:\text{Cr}^{3+}$  and 0.791 for  $\text{ZnGa}_2\text{O}_4:\text{Cr}^{3+}$ , respectively. The “scaled” energy level sets are also shown in Table 3.

The value of the scaling factor, as seen from the above data, depends on the host. Besides, as shown in [23] for free trivalent rare-earth ions, this factor is also ion-dependent. To estimate its value for any system the knowledge of the experimental absorption spectrum is required, but from the results of the previous calculations the limits of its variation can be established to be between 0.6 and 0.9 approximately.

Since the actual symmetry of the considered clusters is not cubic, orbital triplets and doublets are split by the low-symmetry component of crystal field. Besides, these energy levels are further split by the spin-orbit interaction. To make comparison with experimental results easier, we calculated the averaged values (centers of gravity) of the groups of levels arising from the split levels. These baricenters should correspond to the positions of the energy levels in an ideal cubic field, and, therefore, can be directly compared with those reported in [7]. Since absorption bands of  $\text{Cr}^{3+}$  ion in both crystals are broad [4–7], agreement between the “scaled” calculated and measured energy levels is satisfactory.

Detailed consideration of the  $\text{ZnAl}_2\text{S}_4:\text{Cr}^{3+}$  energy levels shows that the order of the observed and calculated  $^4\text{T}_{2g}$  and  $^2\text{T}_{2g}$  is inverted (Tab. 3). The  $^2\text{T}_{2g}$  level in [4–7] is reported to be below the  $^4\text{T}_{2g}$  level, whereas the calculated in the present work values do not support this conclusion. To clarify this situation, additional independent checking using the Tanabe-Sugano matrices for a cubic crystal field [27,29,30] was performed. The values of Racah parameters  $B$  and  $C$  reported in [7] ( $700\text{ cm}^{-1}$  and  $3214\text{ cm}^{-1}$ ) as well as the value of the crystal field strength  $Dq$   $1620\text{ cm}^{-1}$  [7] were used for the calculations of the  $\text{ZnAl}_2\text{S}_4:\text{Cr}^{3+}$  energy levels in cubic approximation. Usage of the reported in [7] values for  $B$ ,  $C$  and  $Dq$  assures the consistency of this checking. Table 4 shows the results of these calculations (only the levels of interest are shown in the table for the sake of brevity).

It is seen that the  $^2\text{T}_{2g}$  level is about  $5800\text{ cm}^{-1}$  higher than the  $^4\text{T}_{2g}$  level, in accordance with the results of DV-ME calculations. Therefore, the energy levels assignment in [4–7] questioned in Table 3 seems to be incorrect. Regarding the origin of the level observed at  $15160\text{ cm}^{-1}$  we propose that this level arises from the  $^4\text{T}_{2g}$  state after it is split by the trigonal crystal field. This suggestion is feasible, since the low-symmetry splitting of the orbital triplet can be of the order of several thousand  $\text{cm}^{-1}$ ; this was confirmed by experimental measurements (e.g. [31,32]) and crystal field calculations (e.g. [33,34]).

Figures 1 and 2 show the calculated (this work) and measured [4] absorption spectra of  $\text{ZnAl}_2\text{S}_4:\text{Cr}^{3+}$ , respectively.

Figures 3 and 4 show the calculated (this work) and measured [10] absorption spectra of  $\text{ZnGa}_2\text{O}_4:\text{Cr}^{3+}$ , respectively.

**Table 3.** Observed and calculated (this work) energy levels (in  $\text{cm}^{-1}$ ) of  $\text{Cr}^{3+}$  ion in  $\text{ZnAl}_2\text{S}_4$  and  $\text{ZnGa}_2\text{O}_4$ .

| $\text{ZnAl}_2\text{S}_4:\text{Cr}^{3+}$ |              |                                     |                                  | $\text{ZnGa}_2\text{O}_4:\text{Cr}^{3+}$ |                            |                                     |                                  |
|--|--------------|-------------------------------------|----------------------------------|--|----------------------------|-------------------------------------|----------------------------------|
| Energy levels                            | Observed [7] | Calculated (without scaling factor) | Calculated (with scaling factor) | Energy levels                            | Observed [10] (baincenter) | Calculated (without scaling factor) | Calculated (with scaling factor) |
| $^4\text{A}_{2g}$                        | 0            | 0                                   | 0                                | $^4\text{A}_{2g}$                        | 0                          | 0                                   | 0                                |
| $^2\text{E}_g$                           | 12 970       | 18 138                              | 12 238                           | $^2\text{E}_g$                           | 14 568                     | 18 779                              | 14 854                           |
| $^2\text{T}_{1g}$                        | 13 170       | 19 068                              | 12 865                           | $^2\text{T}_{1g}$                        | –                          | 19 834                              | 15 689                           |
| $^2\text{T}_{2g}$                        | 15 160*      | 28 014                              | 18 901                           | $^4\text{T}_{2g}$                        | 18 400                     | 21 468                              | 16 981                           |
| $^4\text{T}_{2g}$                        | 16 200       | 22 949                              | 15 484                           | $^2\text{T}_{2g}$                        | 22 000                     | 28 697                              | 22 699                           |
| $^4\text{T}_{1g}$                        | 20 260       | 31 698                              | 21 386                           | $^4\text{T}_{1g}$                        | 24 250                     | 30 841                              | 24 395                           |

\* Assignment is questioned in the text.

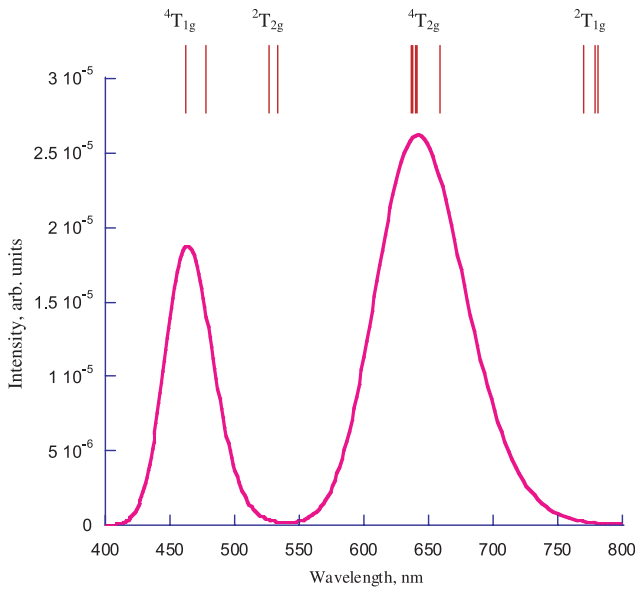


**Fig. 1.** Calculated absorption spectrum of  $\text{ZnAl}_2\text{S}_4:\text{Cr}^{3+}$ . Those multiplets of  $\text{Cr}^{3+}$  ion contributing to the spectrum are shown at the top of the figure.

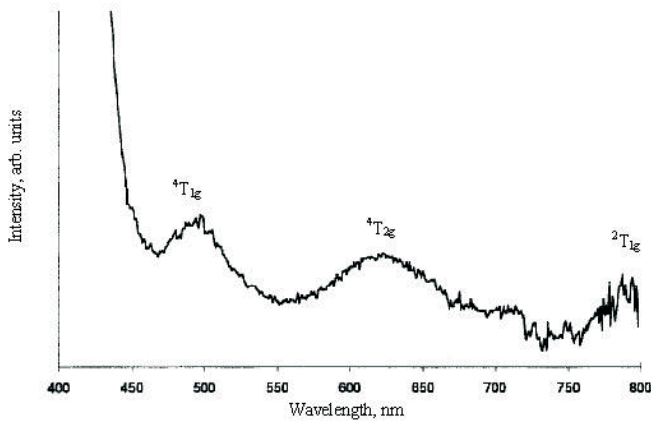
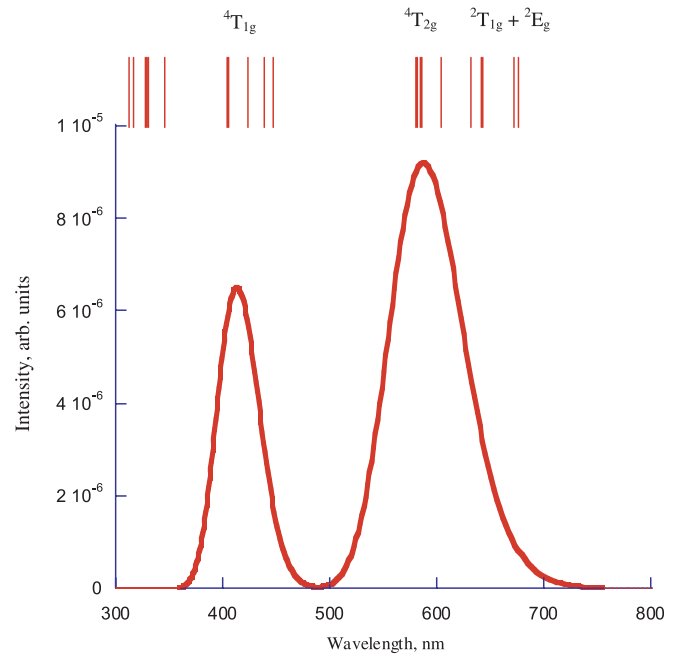


Fig. 2. Experimental absorption spectrum of  $\text{ZnAl}_2\text{S}_4:\text{Cr}^{3+}$  at 295 K (after [4]).

**Fig. 2.** Experimental absorption spectrum of  $\text{ZnAl}_2\text{S}_4:\text{Cr}^{3+}$  at 295 K (after [4]).

**Table 4.** Energy levels (in  $\text{cm}^{-1}$ ) of  $\text{Cr}^{3+}$  ion in  $\text{ZnAl}_2\text{S}_4$  calculated using the Tanabe-Sugano matrices [27,30,31] with parameters  $B = 700 \text{ cm}^{-1}$ ,  $C = 3214 \text{ cm}^{-1}$ , and  $Dq = 1620 \text{ cm}^{-1}$ . Only levels observed in [4–7] are shown.

| $O_h$ group irreducible representation | Energy |
|--|--------|
| $^4\text{A}_{2g}$                      | 0      |
| $^2\text{E}$                           | 14 773 |
| $^2\text{T}_{1g}$                      | 15 397 |
| $^4\text{T}_{2g}$                      | 16 200 |
| $^2\text{T}_{2g}$                      | 22 046 |
| $^4\text{T}_{1g}$                      | 23 058 |
| ...                                    | ...    |



**Fig. 3.** Calculated absorption spectrum of  $\text{ZnGa}_2\text{O}_4:\text{Cr}^{3+}$ . Those multiplets of  $\text{Cr}^{3+}$  ion contributing to the spectrum are shown at the top of the figure.

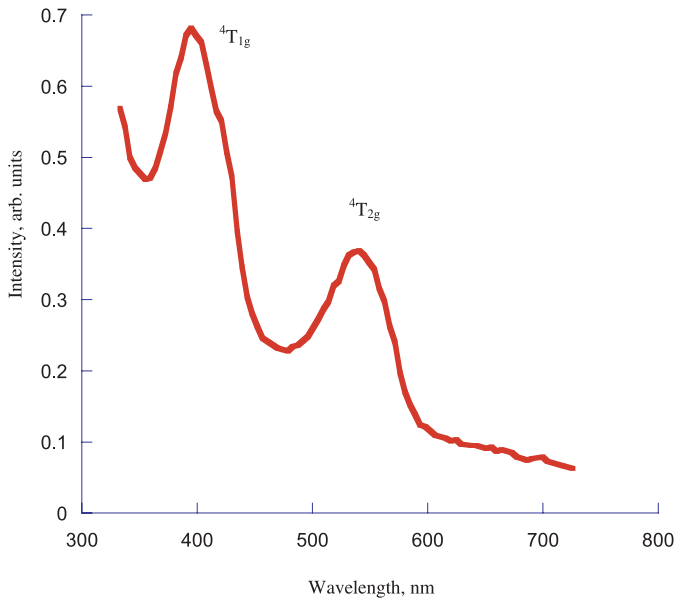


**Fig. 4.** Experimental absorption spectrum of  $\text{ZnGa}_2\text{O}_4:\text{Cr}^{3+}$  at 77 K (after [10]).

**Table 5.** Partial contributions (in %) of atomic  $3d$ -orbitals from  $\text{Cr}^{3+}$  and  $3p$ - and  $3s$ -orbitals from  $\text{S}^{2-}$  to the  $3d$  MO's in the octahedral  $[\text{CrS}_6]^{9-}$  cluster ( $\text{ZnAl}_2\text{S}_4$ ).

|                 | $\text{Cr}^{3+}$ $3d$ -orbitals | $\text{S}^{2-}$ $3p$ -orbitals | $\text{S}^{2-}$ $3s$ -orbitals |
|-----------------|---------------------------------|--------------------------------|--------------------------------|
|                 | 97.18                           | 2.82                           | 0.00                           |
| $t_{2g}$ levels | 97.08                           | 2.91                           | 0.00                           |
|                 | 97.06                           | 2.94                           | 0.00                           |
| $e_g$ levels    | 77.12                           | 20.87                          | 2.00                           |
|                 | 77.11                           | 20.89                          | 2.00                           |
| Averaged        | 89.11                           | 10.09                          | 0.80                           |

The spectra were obtained by using equation (3); the computed “stick” spectra were then broadened by a Gaussian function. The calculated multiplet structures of  $\text{Cr}^{3+}$  ions in both crystals (those which contribute effectively to the spectra) are shown at the top of the figures.

Agreement between the calculated and measured spectra is satisfactory, especially taking into account wide absorption bands and overlapping of absorption bands arising from different multiplets in experimental spectra (Figs. 2 and 4).

It is interesting to compare the covalency effects in both crystals. This can be done by performing the Mulliken's population analysis [35] of the MO, the main results of which are summarized in Tables 5 and 6.

The averaged contribution of the sulfur  $3p$ -orbitals into the  $3d$  MO in  $\text{ZnAl}_2\text{S}_4$  is about 10.09% (Tab. 5), whereas the same quantity for the oxygen  $2p$ -orbitals in  $\text{ZnGa}_2\text{O}_4$  is about 8.20% (Tab. 6). The contribution of the ligands'  $s$  orbitals is also greater in  $\text{ZnAl}_2\text{S}_4$  than in  $\text{ZnGa}_2\text{O}_4$  (0.80% and 0.48%, respectively). These numbers show that the covalency effects are more significant in  $\text{ZnAl}_2\text{S}_4$  crystal than in  $\text{ZnGa}_2\text{O}_4$ , even if the “ $\text{Cr}^{3+}$ -ligand” dis-

**Table 6.** Partial contributions (in %) of atomic  $3d$ -orbitals from  $\text{Cr}^{3+}$  and  $2p$ - and  $2s$ -orbitals from  $\text{O}^{2-}$  to the  $3d$  MO's in the octahedral  $[\text{CrO}_6]^{9-}$  cluster ( $\text{ZnGa}_2\text{O}_4$ ).

|                 | $\text{Cr}^{3+}$ $3d$ -orbitals | $\text{O}^{2-}$ $2p$ -orbitals | $\text{O}^{2-}$ $2s$ -orbitals |
|-----------------|---------------------------------|--------------------------------|--------------------------------|
|                 | 96.30                           | 3.70                           | 0.00                           |
| $t_{2g}$ levels | 96.45                           | 3.55                           | 0.00                           |
|                 | 96.43                           | 3.57                           | 0.00                           |
| $e_g$ levels    | 83.74                           | 15.07                          | 1.19                           |
|                 | 83.72                           | 15.09                          | 1.19                           |
| Averaged        | 91.33                           | 8.20                           | 0.48                           |

tance in this crystal is significantly greater (2.410 Å for  $\text{ZnAl}_2\text{S}_4$  and 1.998 Å for  $\text{ZnGa}_2\text{O}_4$ ).

Since the  $d$ - $d$  transitions are parity forbidden, the contributions of the  $p$ -functions of ligands into the MO make them partially allowed.

The contribution of the ligands'  $p$ - and  $s$ -orbitals to the  $3d$  MO also follows geometric properties of the considered clusters. In the octahedral cluster the  $t_{2g}$  orbitals are directed from the central ion into the space between the ligands, whereas the  $e_g$  orbitals are directed toward ligands. Therefore, the contribution of the ligands' wave functions should be greater in the case of the  $e_g$  orbitals, as confirmed by data in Tables 5 and 6.

## 4 Conclusion

First-principles analysis of the optical spectra of  $\text{Cr}^{3+}$ -doped  $\text{ZnAl}_2\text{S}_4$  and  $\text{ZnGa}_2\text{O}_4$  crystals was performed in the present paper. The energies of the  $\text{Cr}^{3+}$  multiplets in both compounds were computed; their values are in a good agreement with experimental results, if the scaling factor is taken into account. Absorption spectra were modeled for both crystals; the positions of the bands correspond to the measured ones. Previously reported assignment of the  $\text{ZnAl}_2\text{S}_4:\text{Cr}^{3+}$  absorption spectrum has been corrected. Numerical analysis of the MO populations allowed to estimate the covalency effects for both hosts. It was shown that the contribution of the sulfur  $p$ - and  $s$ -orbitals into the  $3d$  MO is greater than that one of the oxygen orbitals.

Fruitful discussions with Associate Professor K. Ogasawara (Kwansei Gakuin University) and members of Computational Materials Science Unit in Kyoto University are gratefully acknowledged.

## References

1. F. Galasso, *Structure and Properties of Inorganic Solids* (Pergamon Press, 1970)
2. M. Wendschuh-Josties, H.S.C. O'Neill, K. Bente, G. Brey, *Neues Jahrbuch für Mineralogie. Monatshefte.* **6**, 273 (1995)

3. H.J. Berthold, K. Koehler, R. Wartchow, *Zeitschrift für Anorganische und Allgemeine Chemie* **496**, 7 (1983)
4. I. Broussell, E. Fortin, L. Kulyuk, S. Popov, *Sol. State Commun.* **99**, 921 (1996)
5. I. Broussell, E. Fortin, L. Kulyuk, S. Popov, V. Tezlevan, *J. Lumin.*, **72–74**, 640 (1997)
6. I. Broussell, E. Fortin, L. Kulyuk, S. Popov, A. Anedda, R. Corpino, *J. Appl. Phys.* **84**, 533 (1998)
7. Z. Mazurak, J. Cisowski, J. Heimann, A. Nateprov, M. Czaja, *Chem. Phys.* **254**, 25 (2000)
8. B. Aktas, S. Guner, F. Yildiz, A. Nateprov, A. Siminel, L. Kulyuk, *J. Magn. Magn. Mater.* **258**, 409 (2003)
9. S. Guner, F. Yildiz, B. Rameev, B. Aktas, *J. Phys.: Condens. Matter* **17**, 3943 (2005)
10. H.M. Kahan, R.M. Macfarlane, *J. Chem. Phys.* **54**, 5197 (1971)
11. J.C.M. Henning, J.P.M. Damen, *Phys. Rev. B* **3**, 3852 (1971)
12. T. Ohtake, N. Sonoyama, T. Sakata, *Chem. Phys. Lett.* **318**, 517 (2000)
13. J.S. Kim, J.S. Kim, T.W. Kim, H.L. Park, Y.G. Kim, S.K. Chang, S. Do Han, *Sol. State Commun.* **131**, 493 (2004)
14. J.S. Kim, J.S. Kim, H.L. Park, *Sol. State Commun.* **131**, 735 (2004)
15. K. Ogasawara, T. Iwata, Y. Koyama, T. Ishii, I. Tanaka, H. Adachi, *Phys. Rev. B* **64**, 115413 (2001)
16. S. Watanabe, H. Kamimura, *Mater. Sci. Eng. B* **3**, 313 (1989)
17. T. Ishii, K. Ogasawara, H. Adachi, I. Tanaka, *J. Chem. Phys.* **115**, 492 (2001)
18. T. Ishii, K. Fujimura, K. Ogasawara, H. Adachi, I. Tanaka, *J. Phys.: Condens. Matter* **13**, 5757 (2001)
19. M.G. Brik, T. Ishii, A.M. Tkachuk, S.E. Ivanova, I.K. Razumova, *J. Alloys Compd.* **374**, 63 (2004)
20. T. Ishii, K. Fujimura, K. Sato, M.G. Brik, K. Ogasawara, *J. Alloys Compd.* **374**, 18 (2004)
21. K. Ogasawara, S. Watanabe, H. Toyoshima, T. Ishii, M.G. Brik, H. Ikeno, I. Tanaka, *J. Sol. State Chem.* **178**, 412 (2005)
22. K. Ogasawara, S. Watanabe, Y. Sakai, H. Toyoshima, T. Ishii, M.G. Brik, I. Tanaka, *Jpn J. Appl. Phys.* **43**, L611 (2004)
23. K. Ogasawara, S. Watanabe, T. Ishii, M.G. Brik, *Jpn J. Appl. Phys.* **44**, 7488 (2005)
24. K. Ogasawara, T. Miyamae, I. Tanaka, H. Adachi, *Mater. Trans.* **43**, 1435 (2002)
25. H. Ikeno, I. Tanaka, L. Miyamae, T. Mishima, H. Adachi, K. Ogasawara, *Mater. Trans.* **45**, 1414 (2004)
26. M.G. Brik, K. Ogasawara, T. Ishii, H. Ikeno, I. Tanaka, *Rad. Phys. Chem.* (accepted)
27. S. Sugano, Y. Tanabe, H. Kamimura, *Multiplets of Transition-Metal Ions in Crystals* (Academic Press, New York, 1970)
28. M.G. Brik, I. Tanaka, T. Ishii, K. Ogasawara, A. Nakamura, S. Watanabe, *J. Alloys Compd.* **408–412**, 753 (2006)
29. W.A. Runcimann, K.A. Schroeder, *Proc. Roy. Soc. (London) A* **265**, 489 (1962)
30. D.T. Sviridov, Yu.F. Smirnov, *Theory of Optical Spectra of Transition Metal Ions* (Nauka, Moscow, 1977) (in Russian)
31. S. Kück, S. Hartung, *Chem. Phys.* **240**, 387 (1999)
32. H. Eilers, U. Hömmerich, S.M. Jacobsen, W.M. Yen, K.R. Hoffman, W. Jia, *Phys. Rev. B* **49**, 15505 (1994)
33. M.G. Brik, N.M. Avram, *Z. Naturforsch. a* **59**, 799 (2004)
34. M.G. Brik, N.M. Avram, C.N. Avram, I. Tanaka, *Eur. Phys. J. Appl. Phys.* **29**, 239 (2005)
35. R.S. Mulliken, *J. Chem. Phys.* **23**, 1833 (1955)